



## Cyclization of 1,5-Dinitrile Systems with Hydrogen Halides: A Search for the Undetected Key Tautomer

Jordi Teixidó,<sup>\*,a</sup> José I. Borrell,<sup>a</sup> Blanca Serra,<sup>a</sup> Carles Colominas,<sup>a</sup> Xavier Batllori,<sup>a</sup> Joan F. Piniella,<sup>b</sup>  
and Angel Alvarez-Larena<sup>b</sup>

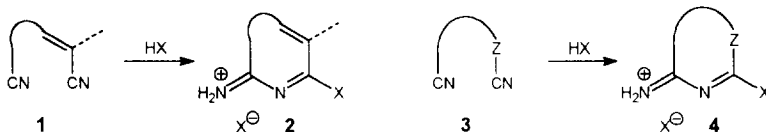
<sup>a</sup>Departament de Química Orgànica, Institut Químic de Sarrià, Universitat Ramon Llull, Via Augusta 390.

E-08017 Barcelona, Spain

<sup>b</sup>Àrea de Cristal·lografia, Universitat Autònoma de Barcelona, E-08193 Bellaterra, Spain

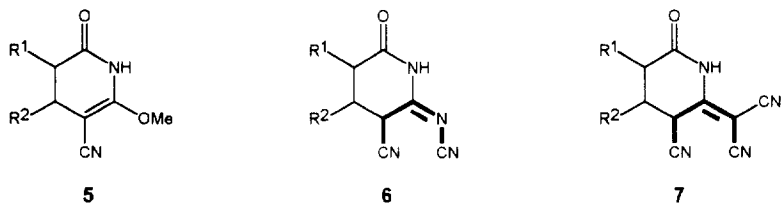
**Abstract:** The  $^{13}\text{C}$  NMR spectra of the pyridones **7a-d** recorded in  $\text{DMSO-d}_6$  show three groups of signals which correspond to the two diastereomers of the **7-exo** tautomer and the **7-endo** tautomer. The X-ray powder analysis and the molecular structures of **7a-c** clearly prove that these compounds, and probably **7d**, are present in the solid state as a single diastereomer of the **7-exo** tautomer which, on being dissolved, establishes an equilibrium with the other diastereomer through the **7-endo** tautomer. This later had been proposed as a key intermediate in the cyclization of the 1,5-dinitrile system present in **7a-d** but was not previously detected. © 1997 Elsevier Science Ltd.

The cyclizations of  $\alpha,\omega$ -dinitriles under the influence of anhydrous hydrogen halides have received a considerable amount of attention due to their wide use for the synthesis of heterocycles.<sup>1</sup> The nature of the internitrile chain determines the direction of cyclization. Thus in those systems which present a cyano group bonded to a  $sp^3$  carbon and a second cyano group bonded to a  $sp^2$  carbon (**1**) or to an heteroatom (**3**), the carbon atom of this later nitrile always bears the halogen atom in the cyclized products (**2**) and (**4**).<sup>2</sup>

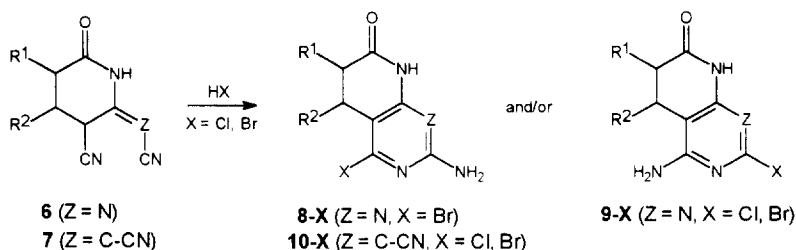


The direction of cyclization of  $\alpha,\omega$ -dinitriles other than those in the above categories has not been predictable. Nevertheless, some interesting works have afforded information about the influence of substitution<sup>3,4</sup> or steric hindrance<sup>5</sup> on the direction of cyclization of some 1-cyanoamino-2,2-dicyanoethylenes and 3-cyanoamino-2-benzenesulphonylbutenedinitriles in the presence of hydrogen chloride.

The cyclization of 1,5-dinitriles with hydrogen halides has been one of the main topics of research of our group<sup>6</sup> since we obtained compounds **6** and **7**, by reaction of the corresponding 2-methoxy-6-oxo-1,4,5,6-tetrahydropyridine-3-carbonitriles (**5**) with  $\text{Na}^+ \text{NC-HZ}^-$ , sodium cyanamide<sup>7</sup> ( $\text{Z} = \text{N}$ ) and malonodinitrile<sup>8</sup> ( $\text{Z} = \text{C-CN}$ ) respectively, which present such kind of substructure.



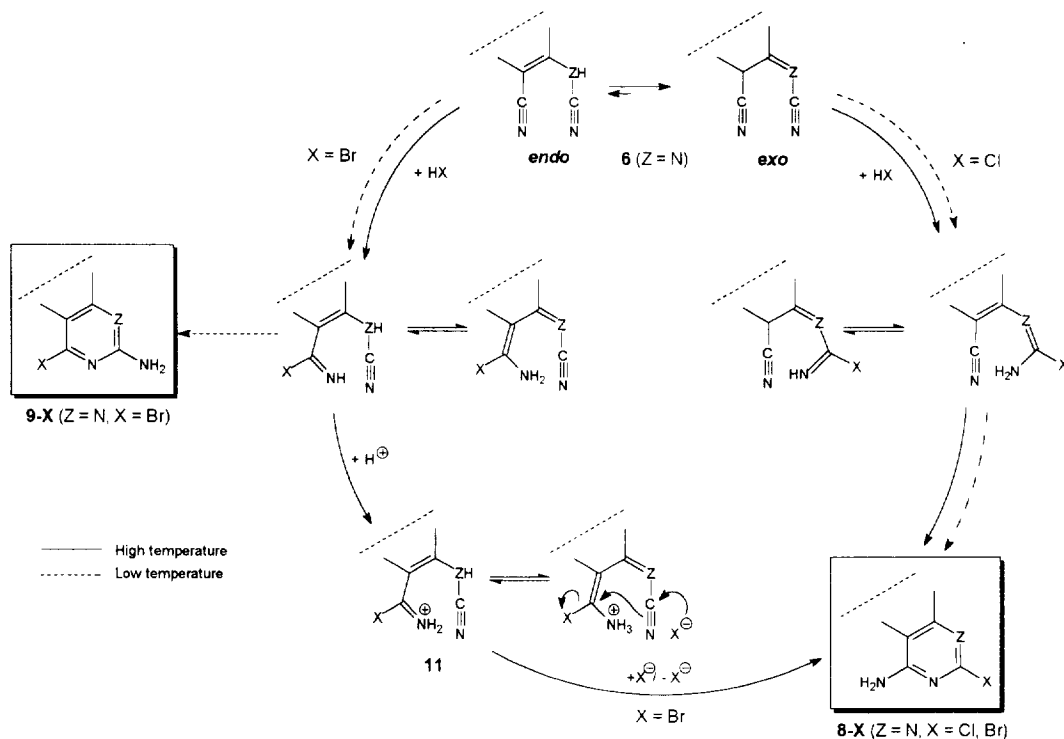
The results obtained in such study mainly depend on the nature of the substrate. When pyridones **6** ( $\text{Z} = \text{N}$ ) were treated with hydrogen chloride using dioxane as solvent, the 4-amino-2-chloro-5,6-dihydropyrido[2,3-*d*]pyrimidin-7(8*H*)-ones (**9-Cl**) were obtained both at low (10-15°C) and high (95-100°C) temperature.<sup>9</sup> However, the treatment of **6** with hydrogen bromide afforded both the positional isomers **8-Br** and **9-Br** depending on the thermal level employed.<sup>10</sup> Thus, when the reaction was carried out at low temperature the 2-amino-4-bromo-5,6-dihydropyrido[2,3-*d*]pyrimidin-7(8*H*)-ones (**8-Br**) were selectively formed, but when it was done at high temperature the 4-amino-2-bromo-substituted compounds (**9-Br**) were predominantly obtained. This behavior was shown to be independent of the nature and position of the substituents present on the pyridone ring.



On the other hand, the dicyanomethylene-substituted pyridones **7** ( $\text{Z} = \text{C-CN}$ ) underwent cyclization with hydrogen halides (HCl or HBr in dioxane/benzene) to afford the 7-amino-5-halo-8-cyano-1,2,3,4-tetrahydro-1,6-naphthyridin-2-ones (**10-X**,  $\text{X} = \text{Cl, Br}$ ), the direction of the cyclization being independent of the temperature and the nature and position of the substituents  $\text{R}^1$  and  $\text{R}^2$ .<sup>8</sup>

In order to explain such results a mechanistic hypothesis (Scheme 1), currently under reinvestigation, was proposed for the cyclization of pyridones **6** ( $\text{Z} = \text{N}$ ) which was based on three factors: kinetic control in the **6-endo**  $\rightleftharpoons$  **6-exo** tautomerism, initial protonation on the most basic cyano group involved in the cyclization (which is the  $\text{C}=\text{Z-CN}$  group in **6-exo** and the  $\text{C}=\text{C-CN}$  group in the **6-endo** tautomer), and two possible reaction paths.<sup>11</sup> According to this hypothesis the formation of **9-Br** would proceed through the protonation of

the C=C-CN group in the **6-endo** tautomer. Even the formation of **8-Br** at high temperature could be rationalized through the **6-endo** tautomer if an addition-elimination mechanism through a protonated imidoyl halide (**11**) is accepted.



*Scheme 1*

The results obtained for the cyclization of compounds **7** (Z = C-CN), examined in the light of the previous mechanistic hypothesis, suggested that the reaction only proceeds through an **7-endo** tautomer independently of the temperature and the hydrogen halide employed. However, the corresponding **endo** tautomers were never detected in solution in the case of compounds **6** (Z = N) and **7** (Z = C-CN).

Consequently, in order to prove the validity of our mechanistic hypothesis we started a search for this undetected key tautomer. The present paper covers the results obtained in such study.

## Results and Discussion

First of all, a calculation of the  $\Delta G^\circ$  of the **endo**  $\rightleftharpoons$  **exo** tautomerism for compounds **6a,b** and **7a,b** was made to evaluate the displacement of the tautomeric equilibrium. The calculation was carried out by using AM1 semiempirical method<sup>12</sup> included in the AMPAC program<sup>13</sup> taking into account two initial considerations:

- a) The **endo** tautomers of compounds **6a,b** and **7a,b** show a single chiral center which corresponds to

the carbon atom which bears the  $R^1$  or  $R^2$  substituent. The final energy value obtained in the optimization of each enantiomer should necessarily be the same. Similarly, the optimization of the same molecule starting from different geometries should lead to the same minimum to give the same energy value.

b) On the other hand, the *exo* tautomers of compounds **6a,b** and **7a,b** present two chiral centers, the carbon atom bearing the  $R^1$  or  $R^2$  substituent and the  $\alpha$ -cyano carbon. The calculations have been carried out for the two configurations of the carbon atom which bears the substituent while the configuration of the  $\alpha$ -cyano carbon is kept fixed,  $5(S)$  in the case of **6a,b** and  $5(R)$  in **7a,b**. The results obtained for  $\Delta G^\circ$  in tautomerism of compounds **6a,b** and **7a,b** are summarized in Table 1.

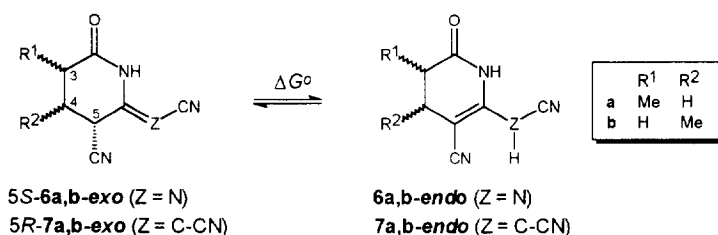


Table 1.  $\Delta G^\circ$  for the *endo*  $\rightleftharpoons$  *exo* tautomerism in **6a,b** and **7a,b**

	$R^1$	$R^2$	$\Delta G^\circ$ (a)
3 <i>R</i> - <b>6a</b>	Me	H	2.0
3 <i>S</i> - <b>6a</b>	Me	H	0.6
4 <i>R</i> - <b>6b</b>	H	Me	2.6
4 <i>S</i> - <b>6b</b>	H	Me	2.2
3 <i>R</i> - <b>7a</b>	Me	H	1.5
3 <i>S</i> - <b>7a</b>	Me	H	0.1
4 <i>R</i> - <b>7b</b>	H	Me	0.6
4 <i>S</i> - <b>7b</b>	H	Me	1.5

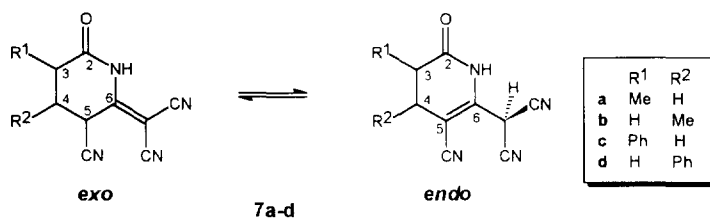
a) Kcal/mol,  $\Delta G^\circ = \Delta G^\circ_{\text{f}}(\text{endo}) - \Delta G^\circ_{\text{f}}(\text{exo})$ .

These results agree with the fact that the tautomeric equilibrium in compounds **6** and **7** lies well to the *exo* form in all cases but the *endo* content seems to be high enough to be detectable by spectroscopic methods.

Consequently, we decided to make a careful revision of the  $^{13}\text{C}$  NMR spectra of compounds **6** and **7** in order to try to detect the corresponding *endo* tautomers by running overnight acquisitions (20 000–30 000 transients) and recording the spectra in  $\text{MeOH-d}_4$ ,  $\text{acetone-d}_6$  and  $\text{DMSO-d}_6$ . In this way, compounds **6** ( $Z = N$ ) gave complex spectra of difficult assignment due to the presence of a mixture of compounds caused by the existence of two chiral centers in the *6-exo* tautomer, the *cis-trans* isomerism of the cyanoimino group present in the *6-exo* tautomer and, possibly, the *endo*  $\rightleftharpoons$  *exo* tautomerism.

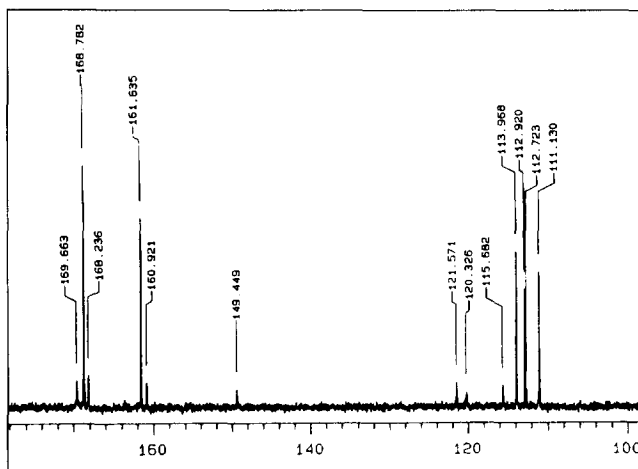
However, the  $^{13}\text{C}$  NMR spectrum of **7b** ( $R^1 = \text{H}$ ,  $R^2 = \text{Me}$ ) recorded in  $\text{DMSO-d}_6$  showed three groups

of signals which correspond to the two pairs of enantiomers of the **7b-exo** tautomer, formed by the presence of two chiral centers (C3 and C5) in this compound, and the **7b-endo** tautomer (Fig. 1). The existence of this later was undoubtedly established by the presence of three signals at 70.8, 149.4, and 27.8 ppm which respectively correspond to C5, C6, and C(CN)<sub>2</sub> of **7b-endo**.



The two diastereomers of **7b-exo** are present in different proportions: the major was assigned to the *4R5R* and *4S5S* enantiomers and the minor to the *4R5S* and *4S5R* pair. These assignments will be discussed later.

Fig. 1. <sup>13</sup>C NMR spectrum of **7b** (expanded plot of the portion 100-180 ppm)

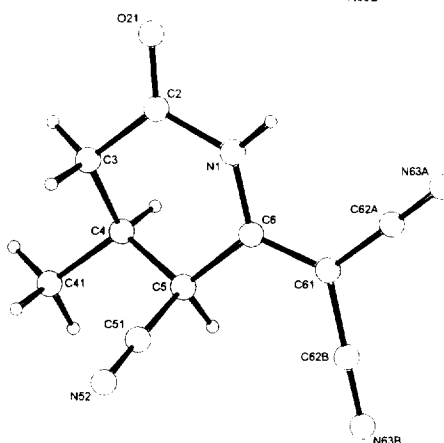
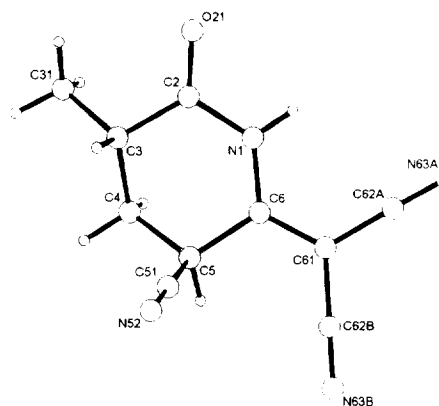
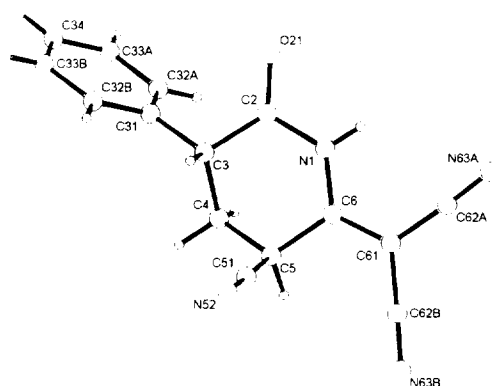
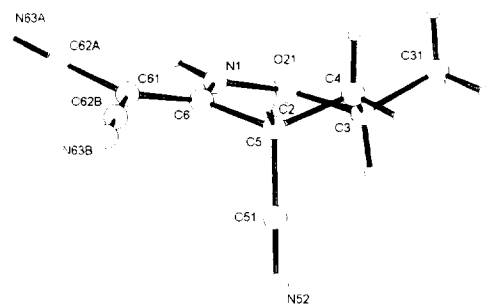


The same behavior was also found in the <sup>13</sup>C NMR spectra compounds **7a** (R<sup>1</sup> = Me, R<sup>2</sup> = H), **7c** (R<sup>1</sup> = Ph, R<sup>2</sup> = H), and **7d** (R<sup>1</sup> = H, R<sup>2</sup> = Ph) when they were recorded in DMSO-d<sub>6</sub>. On the contrary, the **endo** tautomer was never detected when the spectra were recorded in MeOH-d<sub>4</sub> or acetone-d<sub>6</sub>. The <sup>13</sup>C NMR spectral data of the **exo** and **endo** tautomers of **7a-d** are summarized in Table 2, some of the assignments have been carried out by using the DEPT spectrum and the DEPT spectrum of the H,D-exchanged compounds.

Recrystallization of **7a** and **7b** from methanol, and from acetonitrile in the case of **7c**, afforded single crystals suitable for an X-ray diffraction study. The structure determination revealed the presence, in all three cases, of only one diastereomer of the **7-exo** tautomers (Figures 2, 3, and 4).

**Table 2.**  $^{13}\text{C}$  NMR data of the *exo* and *endo* tautomers of 7a-d.

	7a			7b			7c			7d		
	<i>exo</i>		<i>endo</i>	<i>exo</i>		<i>endo</i>	<i>exo</i>		<i>endo</i>	<i>exo</i>		<i>endo</i>
	<i>RS-SR</i>	<i>RR-SS</i>		<i>RR-SS</i>	<i>RS-SR</i>		<i>RS-SR</i>	<i>RR-SS</i>		<i>RR-SS</i>	<i>RS-SR</i>	
C2	171.8	172.0	173.0	168.8	168.2	169.7	170.1	169.1	170.8	169.1	169.1	168.5
C3	32.9	33.8	35.5	35.6	35.6	35.6	44.4	45.0	46.9	32.7	32.6	30.8
C4	28.3	28.1	30.5	34.5	34.1	35.6	28.5	29.3	30.6	35.8	35.8	35.4
C5	29.0	29.2	63.6	26.9	29.1	70.8	29.2	29.2	63.6	36.4	36.4	63.0
C6	162.2	162.9	150.1	161.6	160.9	149.4	161.9	160.2	150.3	161.3	161.5	150.1
C(CN) <sub>2</sub>	61.2	62.0	28.2	61.7	63.0	27.8	61.7	62.9	28.5	62.1	68.1	38.8
CN	116.1	116.4	121.6	114.0	115.7	120.4	116.0	114.4	121.6	113.9	115.2	121.4
	113.1	112.8	121.2	112.9	112.7	121.6	113.1	111.8	119.2	113.0	112.6	121.0
	111.3	111.7		111.1			111.3	111.5		111.2	111.4	
R	14.5 (Me)	14.7 (Me)	14.4 (Me)	17.3 (Me)	17.5 (Me)	19.3 (Me)	136.9 <i>ipsoPh</i>	135.4 <i>ipsoPh</i>	138.3 <i>ipsoPh</i>	136.8 <i>ipsoPh</i>	137.8 <i>ipsoPh</i>	137.5 <i>ipsoPh</i>

**Figure 3.** Molecular structure of (4S,5S)-7b-*exo* (PC-PLUTO<sup>15</sup>)**Figure 2.** Molecular structure of (3S,5S)-7a-*exo* (frontal and lateral views) (PC-PLUTO<sup>15</sup>)**Figure 4.** Molecular structure of (3R,5S)-7c-*exo* (PC-PLUTO<sup>15</sup>)

The molecular structures of three compounds analyzed are quite similar and show the same spatial disposition. The **7-exo** tautomer nature is unequivocally established by the tetrahedral arrangement around C5, the trigonal nature of C6, and by the C6-C61 bond length (1.357(2), 1.365(2) and 1.354(3) for **7a**, **7b** and **7c** respectively) and the C5-C6 distance (1.517(2), 1.513(2) and 1.516(3) for **7a**, **7b** and **7c** respectively) which correspond to a double and single bond respectively. The cyano group linked to C5 shows a *quasi-axial* position while the substituent present in C3 (Me in **7a** or Ph in **7c**) or C4 (Me in **7b**) is always in an *equatorial* position. Finally, the pyridone ring present in compounds **7a-c** shows a *pseudo-sofa* conformation with a C3-C2-N1-C6-C5 planar region from which C4 deviates.

In the three crystals studied the space group is centrosymmetric and two enantiomers are present. In the case of **7a**, the two enantiomers form a dimer through a double hydrogen bond between the NH and carbonyl groups of each enantiomer (NH $\cdots$ OC, 2.12(2) Å; N $\cdots$ O, 2.919(2) Å; N-H $\cdots$ O, 151(1) $^\circ$ ). This kind of association was previously observed in the case of **5a** (R<sup>1</sup> = Me, R<sup>2</sup> = H).<sup>14</sup>

Compound **7b** also shows a dimeric association of the two enantiomers present but the hydrogen bridge is formed between the NH and one of the cyano groups of the dicyanomethylene unit (NH $\cdots$ NC, 2.22(2) Å; N $\cdots$ N, 3.086(2) Å; N-H $\cdots$ N, 164(1) $^\circ$ ). Finally, in the case of **7c** each enantiomer is associated in a chain through a single hydrogen bond between the NH group of one molecule and a cyano group of the dicyanomethylene unit of the next molecule (NH $\cdots$ NC, 2.46(2) Å; N $\cdots$ N, 3.225(5) Å; N-H $\cdots$ N, 152(2) $^\circ$ ).

In order to confirm, excluding any possible sampling error, the existence of compounds **7a-c** in the solid state only as one diastereomer of the corresponding **7-exo** tautomer, the X-ray powder diffraction patterns were experimentally determined for **7a-c** and calculated from single crystal data.<sup>16</sup> As an example Figure 5 and Figure 6 show the experimental and calculated powder diffraction data of **7b**. Comparison of the experimental and calculated patterns allowed the indexation of all the experimental peaks. Consequently, the aforementioned **7-exo** diastereomers, the structures of which were determined by single crystal X-ray diffraction, are predominant in the solid state. The concentrations of the other **7-exo** diastereomer and the **7-endo** tautomer, if any, are below the detection limit.

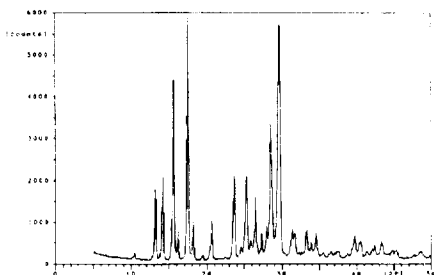


Figure 5. Experimental powder diffraction pattern of **7b**

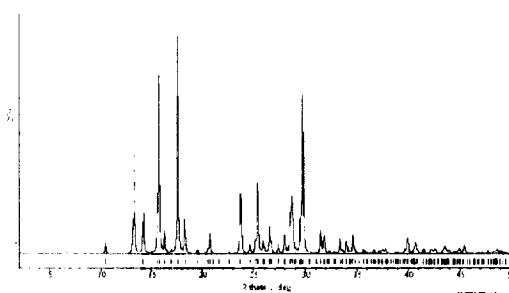


Figure 6. Calculated powder diffraction pattern of **7b** (POWDER CELL 1.8a<sup>16</sup>)

This result clearly proves that compounds **7a-c**, and probably **7d**, are present in the crystals obtained from methanol as a single diastereomer of the **7-*exo*** tautomer which, on being dissolved in DMSO, establishes an equilibrium with the other diastereomer through the **7-*endo*** tautomer as the  $^{13}\text{C}$  NMR spectral data shown.

A final remarkable aspect of the present study is the fact that the semiempirical (AM1, PM3) and *ab-initio* (HF/6-31G\*) calculations carried out on compounds **7a-d** gave, as the most stable structure, the same diastereomer found in the solid state, the calculated geometry being almost superimposable with that present on the single crystals. Thus Table 3 shows selected bond lengths and angles of **7b** determined by X-ray diffraction and calculated by semiempirical and *ab-initio* methods.

Bond lengths	X-Ray	AM1	PM3	HF/6-31G*	Bond angles	X-Ray	AM1	PM3	HF/6-31G*
C2-C3	1.480(2)	1.51	1.51	1.51	C2-C3-C4	113.6(1)	112.1	112.1	113.2
C2-O21	1.206(2)	1.24	1.22	1.19	C2-N1-C6	126.5(1)	124.2	123.2	127.8
C3-C4	1.510(2)	1.52	1.52	1.53	C3-C4-C41	111.9(1)	110.9	110.4	112.3
C4-C41	1.521(2)	1.51	1.52	1.53	C3-C4-C5	109.2(1)	110.1	110.5	109.2
C4-C5	1.534(2)	1.53	1.54	1.55	C4-C5-C51	112.4(1)	111.9	112.4	111.7
C5-C51	1.466(2)	1.45	1.46	1.48	C4-C5-C6	112.0(1)	110.3	110.7	110.3
C5-C6	1.513(2)	1.52	1.52	1.52	C41-C4-C5	111.9(1)	111.3	111.8	112.3
C51-C52	1.134(2)	1.16	1.16	1.13	C5-C51-C52	177.6(2)	179.2	179.0	178.7
C6-C61	1.365(2)	1.38	1.37	1.35	C5-C6-C61	120.3(1)	119.8	121.5	121.8
C61-C62A	1.427(2)	1.42	1.42	1.44	C51-C5-C6	109.2(1)	109.4	108.7	108.9
C61-C62B	1.425(2)	1.42	1.42	1.43	C6-C61-C62A	122.2(1)	122.1	122.7	120.4
C62A-N63A	1.143(2)	1.16	1.16	1.14	C6-C61-C62B	120.8(1)	121.9	122.2	121.6
C62B-N63B	1.139(2)	1.16	1.16	1.14	C61-C62A-N63A	179.0(2)	179.6	178.7	177.0
N1-C2	1.340(2)	1.41	1.43	1.40	C61-C62B-N63B	179.2(2)	178.8	178.9	178.8
N1-C6	1.351(2)	1.38	1.41	1.36	C62A-C61-C62B	117.0(1)	116.0	115.1	118.0
<b>Table 3. Experimental (X-Ray) and calculated (AM1, PM3 and HF/6-31G*) selected bond lengths (Å) and bond angles (°) for 7b.</b>					N1-C2-C3	116.5(1)	119.0	119.6	116.7
					N1-C2-O21	118.0(1)	117.9	114.8	119.1
					N1-C6-C5	118.0(1)	118.0	117.6	116.3
					N1-C6-C61	121.7(1)	122.1	120.9	121.9
					O21-C2-C3	125.5(1)	123.2	125.6	124.1

A comparison of the r.m.s. values obtained for the 3D global fits between the X-ray geometry and the calculated ones, AM1 (0.166), PM3 (0.190) and HF/6-31G\* (0.194), indicates that the AM1 method gives the best global fit probably due to a best fitting of the dihedral angles.

The fact that the structures calculated *in vacuo* and those present in the solid state show the same configuration, together with the very low differences between the calculated solvation free energies in water (determined by using the Miertus-Scrocco-Tomasi method<sup>17</sup>) of the **7-*exo*** and the **7-*endo*** tautomers, allow us to consider that the major **7-*exo*** diastereomer present in solution has, in each case, the same configuration.



This assumption let us to assign the configurations of the major and minor diastereomers of **7a-d** depicted in Table 2.

## Experimental Section

**General:** Compounds **6a,b** and **7a-d** were prepared according to reported procedures.<sup>7,8</sup> <sup>1</sup>H and <sup>13</sup>C NMR spectra were recorded on a Varian Gemini 300 spectrometer using TMS as an internal standard.

**Semiempirical calculations:** Semiempirical calculations were carried out on an IBM RISC/6000 workstation running under AIX-3.2. The optimization was performed, starting with a structure constructed with program MAD (Molecular Advanced Design)<sup>18</sup> and initially refined with MM2<sup>19</sup>, by using the AM1 Hamiltonian<sup>12</sup> of the AMPAC 2.1 program<sup>13</sup> included in the MOTECC-91 package.<sup>20</sup> The AM1 options were fixed as follows: PRECISE, FORCE, PULAY, ROT=1, THERMO(298,298,0). The PM3 calculations were carried out by using the PM3 Hamiltonian<sup>21</sup> included in the MOPAC 6.0 program.<sup>22</sup> Solvation free energies were calculated by using the MST (Miertus-Scrocco-Tomasi) method<sup>17</sup> included in MOPAC93 program.<sup>23</sup>

**Ab-initio calculations:** *Ab-initio* calculations were carried out on the same workstation using GAMESS program.<sup>24</sup> Geometry optimizations were performed at Hartree Fock level of theory using 6-31G basis set including polarization functions on heavy atoms (denoted as HF/6-31G\*).

**X-Ray diffraction:** Suitable crystals were grown from methanol solution for **7a** and **7b**, and from an acetonitrile solution for **7c**. Cell constants were obtained by least-squares refinement on diffractometer angles for 25 automatically centered reflections,  $\lambda = 0.71069$  Å, CAD4 diffractometer, room temperature,  $\omega/2\theta$  mode with  $\omega$  scan width =  $0.80 + 0.35 \tan\theta$ ,  $\omega$  scan speed 1.3-5.5 deg min<sup>-1</sup>, graphite-monochromated radiation,  $1 < \theta < 25^\circ$ , Lp but no absorption corrections were applied. Structures were resolved by direct methods (SHELXS-86<sup>25</sup> program) and refined by full-matrix least squares refinement on  $F^2$  for all reflections (SHELXL-93<sup>26</sup> program). No hydrogen atoms were refined anisotropically. Hydrogen atoms in calculated positions with global isotropic temperature factors.<sup>27</sup>

Powder diffraction data were collected at 293 K with a Philips XPert diffractometer operating at 40 kV and 55 mA equipped with a  $\theta/2\theta$  goniometer, a fixed divergence slit of 1°, a receiving slit of 0.10 mm, and a secondary graphite monochromator. Data were recorded using a step size of 0.03° and a collecting time of 1 s. CuK $\alpha$  radiation was used (1.5419 Å).

## Acknowledgments

Support of this work by a grant from the *Comisión Interministerial de Ciencia y Tecnología* and the *Comissió Interdepartamental de Recerca i Innovació Tecnològica* within the *Programa de Química Fina* (QFN93-4420). Two of us (B. S. and C. C.) would like to thank *Fundación Juan Salanyer* and *IBM España* respectively for a grant.

## References and Notes

1. Johnson, F.; Madroñero, R. In *Adv. Heterocycl. Chem.*; Katritzky, A. R. Ed; Academic Press: New York, 1966; Vol. 6, pp. 95-146.
2. Yanagida, S.; Okahara, M.; Komori, S. In *Adv. Org. Chem.*; Böhme, H.; Viehe, H. G. Eds; John Wiley and Sons, Inc, New York, 1979; Vol. 9, part 2, pp. 527-571.
3. Allestein, E.; Fuchs, R. *Chem. Ber.* **1968**, *101*, 1244-1249.
4. Kristinsson, H. *J. Chem. Soc., Chem. Commun.* **1974**, 350.
5. Pérez, M. A.; Soto, J. L.; Gúzman, F.; Alcalá, H. *J. Chem. Soc. Perkin Trans. 1* **1985**, 87-91.

6. Victory, P.; Borrell, J. I. *Trends in Heterocyclic Chemistry* **1993**, *3*, 235-247 and the references cited therein.
7. Victory, P.; Nomen, R.; Colomina, O.; Garriga, M.; Crespo, A. *Heterocycles* **1985**, *23*, 1135-1141.
8. Victory, P.; Teixidó, J.; Borrell, J. I. *Heterocycles* **1992**, *34*, 1905-1916.
9. Victory, P.; Garriga, M. *Heterocycles* **1985**, *23*, 2853-2858.
10. Victory, P.; Garriga, M. *Heterocycles*, **1985**, *23*, 1947-1950.
11. Victory, P.; Garriga, M. *Heterocycles*, **1986**, *24*, 3053-3058.
12. Dewar, M. J. S.; Zoebisch, E. G.; Healy, E. F.; Stewart, J. J. P. *J. Am. Chem. Soc.* **1985**, *107*, 3902-3909.
13. Dewar, M. J. S. *AMPAC 2.1*; Department of Chemistry, University of Florida, Gainesville, FL, 1991.
14. Borrell, J. I.; Teixidó, J.; Martínez-Teipel, B.; Busquets, N.; Serra, B.; Alvarez-Larena, A.; Piniella, J. F. *Afinidad*, **1993**, *50*, 411-419.
15. Schmid, G.; Brueggemann, R. *PC-PLUTO*; University of Ulm, Germany, 1990.
16. Kraus, W.; Nolze, G. *POWDER CELL 1.8a*, Federal Institute for Materials Research and Testing (BAM), Berlin, 1996.
17. a) Miertus, S.; Scrocco, E.; Tomasi, J. *Chem. Phys.*, **1981**, *55*, 117-129. b) Miertus, S.; Tomasi, J. *Chem. Phys.*, **1982**, *65*, 239-245. c) Orozco, M.; Luque, F. J. *Chem. Phys.*, **1994**, *182*, 237-248.
18. Lahana, R. *MAD: Molecular Advanced Design 2.12*; Oxford Molecular Ltd, X-pole École Polytechnique, F-91128 Palaiseau, Cédex; France, 1992.
19. Allinger, N. L. *J. Am. Chem. Soc.* **1987**, *109*, 6283-6289.
20. Clementi, E. *MOTEC-91*; ESCOM Science Publishers B. V., 1991.
21. a) Stewart, J. J. P. *J. Comput. Chem.*, **1989**, *10*, 209-220. b) Stewart, J. J. P. *J. Comput. Chem.*, **1989**, *10*, 221-264.
22. Stewart, J. J. P. *MOPAC 6.0*, QCPE#455.
23. Stewart, J. J. P. *MOPAC93*, Rev. 2, Fujitsu Ltd, 1993.
24. Schmidt, M. W.; Baldridge, K. K.; Boatz, J. A.; Elbert, S. T.; Gordon, M. S.; Jensen, J. J.; Koseki, S.; Matsunaga, N.; Nguyen, K. A.; Su, S.; Windus, T. L.; Dupuis, M.; Montgomery, J. A. *GAMESS v. 2.0*, Apr. 95, *J. Comput. Chem.*, **1993**, *K14K*, 1347-1363.
25. Sheldrick, G. M. *SHELXS-86. Crystallographic Computing 3*, Sheldrick, G. M.; Krüger, C.; Goddard, R. Eds; Oxford University Press, 1985, pp. 175-189.
26. Sheldrick, G. M. *SHELXL-93: Program for the refinement of crystal structures from diffraction data*; Institut für Anorg. Chemie, Göttingen, Germany, 1993.
27. (a) The atomic co-ordinates for this work are available on request from the Director of the Cambridge Crystallographic Data Centre, University Chemical Laboratory, Lensfield Road, Cambridge CB2 1EW. Any request should be accompanied by the full literature citation for this communication. (b) Supplementary data available include crystal data, atomic coordinates, thermal parameters, bond distances and bond angles for the X-ray structures of **7a**, **7b**, and **7c**.

(Received in UK 17 December 1996; revised 27 January 1997; accepted 30 January 1997)